Supporting Information

A nanopore-nanofiber mesh biosensor to control DNA translocation

Allison Squires,[1]‡ Joseph S. Hersey,[1]‡ Mark W. Grinstaff[1, 2]* and Amit Meller[1, 3, 4] *

[1]Departments of Biomedical Engineering, [2]Chemistry, and [3]Physics at Boston University, Boston, Massachusetts, 02215, United States

[4]Faculty of Biomedical Engineering at the Technion, Haifa, 32000, Israel

1) Online Methods

General Procedure and Methods: All chemicals were purchased from Sigma Aldrich and used without further purification, unless otherwise noted. Solvents used during synthesis were dried and distilled prior to use. All reactions were conducted in dry conditions in a nitrogen atmosphere. DCM= dichloromethane and THF= tetrahydrofuran. Chemical shifts are reported in parts per million (ppm) as follows: chemical shift, multiplicity (s= singlet, d= doublet, t= triplet, q= quartet, m= multiplet, br= broad).

PGC-C18 Polymer Synthesis: A Poly(glycerol-co-ε-caprolactone) (1:4) (PGC) backbone was synthesized using a previously published protocol. Specifically the PGC polymer was synthesized through a tin octanoate catalyzed (1/100 eq) ring opening polymerization of the ε-caprolactone and 5-(benzyloxy)-1,3-dioxan-2-one monomers in a 4:1 ratio, respectively, at 140°C for 12 hours. The copolymer was isolated through a precipitation in cold methanol (yield: 99%). The benzyl protecting group was removed from the polymer backbone using a palladium-catalyzed hydrogenation in THF for 16 hours at 50 psi. The catalyst was removed by filtering the product through Celite (yield: 99%). The deprotected PGC polymer (PGC-OH) was dissolved in DCM with stearic acid, N,N'-dicyclohexylcarbodiimide (DCC), and 4-dimethylaminopyridine (DMAP) and stirred at room temperature for 16 hours to functionalize the polymer with stearic acid. Dicyclohexylurea was removed by filtration and the solvent removed by evaporation. The stearic acid functionalized PGC (PGC-C18) was purified by dissolving the polymer in DCM and precipitating it into cold methanol. The PGC-C18 polymer was filtered and dried under hi vacuum for 12 hours (Yield: 93%) (22,000 g/mol, PDI 1.4 by GPC). 1H NMR (400 MHz, $CDCl_3$) (Figure S2): δ= 0.79-0.83 (t, J=8 Hz, 3 H; CH_3), 1.15-1.21 (s, 32 H; CH_2), 1.29-1.35 (m, 4 H; CH_2), 1.56-1.64 (m, 18 H; CH_2), 2.22-2.28 (m, 10 H; CH_2), 3.97-4.01 (t, 8H; CH_2), 4.03-4.34 (m, 6 H; CH_2), 5.17-5.23 (m, 1 H; CH). ^{13}C NMR (400 MHz, $CDCl_3$) (Figure S3): δ= 14.1, 22.7, 24.6, 25.5, 28.3, 29.7, 31.9, 34.1, 62.0, 64.1, 65.5, 68.2, 68.6, 154.85, 172.87, 173.54. [1,2]

Gel permeation chromatography (GPC): PGC-C18 molecular weights were determined by GPC versus polystyrene standards using a THF elutent at a 1.0 mL/min flow rate through a Styragel column (HR4E THF, 7.8 x 300 mm) with a refractive index detector.

Nanopore fabrication and drilling: Nanopore chips are fabricated from a <1,0,0> single-crystal silicon wafer through-etched to leave a thin (~20 nm) freestanding silicon nitride (SiN) membrane supported by a small (5 mm x 5 mm x 0.35 mm) silicon chip.

A nanopore is drilled through the SiN using a highly focused transmission electron microscope beam ($10^8 – 10^9$ e^-/nm^2) to sputter away material from the thin membrane according our previously published method.[3] A sample image of a pore used in this study is shown in Figure S1. Nanopores were drilled and cleaned prior to electrospinning.

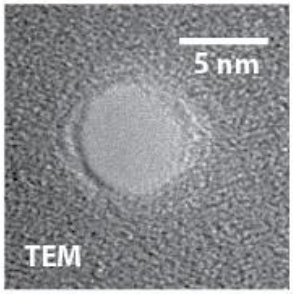

Figure S1. Tunneling Electron Microscope (TEM) image of nanopore taken after drilling

Fabrication of NP-NFMs: The following co-polymer blends were created in 5:1 chloroform:methanol solutions: 7% by wt. poly(ε-caprolactone) (PCL) (70,000-90,000 MW, Sigma) (PCL alone solution), 7% by wt. PCL + 0.78% by wt. PGC-C18 (9:1 PCL:PGC-C18 blend), 7% by wt. PCL + 1.75% by wt. PGC-C18 (8:2 PCL:PGC-C18 blend), 7% by wt. PCL + 3% by wt. PGC-C18 (7:3 PCL:PGC-C18 blend), 7% by wt. PCL + 4.66% PGC-C18 (6:4 PCL:PGC-C18 blend), 7% by wt. PCL + 7% by wt. PGC-C18 (5:5 PCL:PGC-C18 blend). The electrospinning parameters were modified from a previous publication based on PCL.[4,5] The procedure was modified to produce nano-fibers (~300 nm) using a 3 ml/hour flow rate, a 8 kV source, a collector distance of 10 cm, and a 20 gauge needle for all electrospun NFMs. The SiN nanopore chips were affixed to one side of a double sided copper tape and the other side was adhered to the grounded collecting surface. NFMs were electrospun for the appropriate time for each blend such that 5 mg of polymer was electrospun onto the grounded collector.

Contact Angle Analysis: A Kruss DSA100 contact angle goniometer was used to quantify the contact angles of water (4 µl) on the surface of the hybrid NP-NFM devices. Each water droplet was allowed to reach its equilibrium contact angle over 15 seconds before the water contact angle was measured.

Scanning Electron Microscopy: A Zeiss SUPRA 55VP field emission SEM was used to image the surfaces of each NP-NFM. The samples were affixed to an aluminum sample stub using copper tape and were coated with 5 nm of Au/Pd prior to imaging and imaged at an accelerating voltage of 2 kV.

Nanopore Cleaning and Wettability: Nanopore chips are cleaned prior to wetting in a heated 3:1 H_2SO_4:H_2O_2 (piranha) bath for 15 minutes to remove any organic contaminants and improve pore wettability.[6] Chips are then rinsed and stored in DI water until use.

Nanopore Electrical Sensing: Nanopore chips are assembled in a Teflon cell and PDMS is used to seal the edges of the chip to prevent current leakage, according to our previously published protocol.[3] Reservoirs on each side of the membrane are filled with an electrolyte buffer (1M KCl, 10 mM Tris-HCl) and all bubbles are removed manually. The NFM coating may be hydrated using 5% ethanol, if necessary, which may then be rinsed out with a 10x buffer exchange. An Axon 200B amplifier is used to apply a voltage clamp (~300 mV) across the membrane via Ag/AgCl electrodes, and the resulting current is measured.

Nanopore Data Collection: All data are collected using National Instruments A/D data acquisition boards and custom Labview software at a rate of 250 kHz, filtered at 100kHz (unless otherwise specified). Conductance is calculated by measuring current as a function of voltage for -500 mV to +500 mV. The electrolyte buffer used in this study was 1M KCl, 10 mM Tris-Cl, pH 7.5. Typical applied bias for translocations is 300 or 500 mV. Electrical noise is measured both as RMS noise for each voltage applied, and also as a frequency-domain spectrum transformed from a continuously recorded current trace. Only NP-NFM devices that displayed voltage response and noise characteristics very similar to an uncoated nanopore were used in this study.

DNA Samples: All DNA samples used in this study were double stranded DNA fragment length standards purchased from ThermoScientific (NoLimits 1000, 500, 5000, 10000, 20000 bp). DNA was stored in 50 mM KCl + TE buffer until use.

Automated Detection of DNA Translocations: DNA translocations through a nanopore are detected as transient drops in conductance (please see Figure 2). Translocations are identified using a custom Labview program, previously described,[6] and events are later automatically evaluated in Matlab to determine the open pore current I_{open} (unblocked pore), the blockage level I_b ($I_b = I_{block}/I_{open}$), and the time of translocation t_T.

Statistics: *Thousands of translocations were collected for each nanopore condition. The number of events is indicated for each data set. Current levels for individual events are determined using Gaussian fits to all-points histograms. Overall open pore current, conductance changes, blockage levels, and so forth are fits to ensemble histograms, unweighted by event time. Distributions for translocation time, t_T, represent the tail of a Poisson-like distribution[6,7] and are characterized by the timescale of an exponential decay fit. Where multiple populations could be distinguished, this fit used two terms, one for collisions and one for translocations, weighted for counting error. A typical r^2 value is 0.9 or higher for both types of fits.*

2) Polymer Synthesis

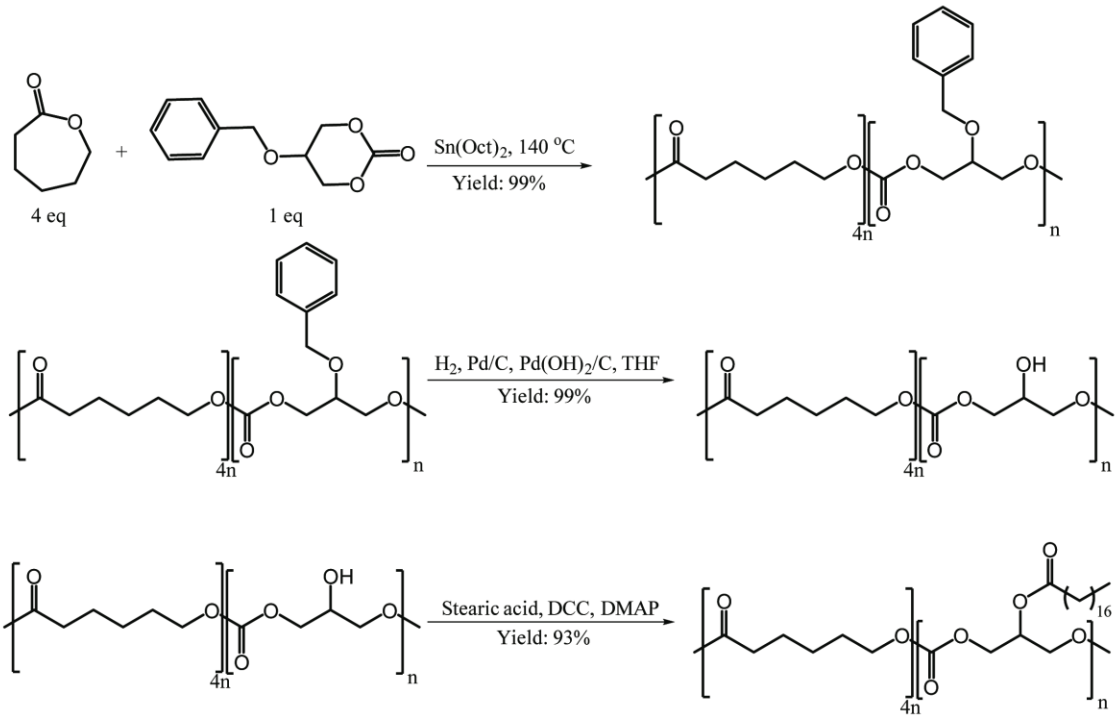

Figure S2. Synthetic scheme of PGC-C18.

3) Polymer Characterization by NMR:

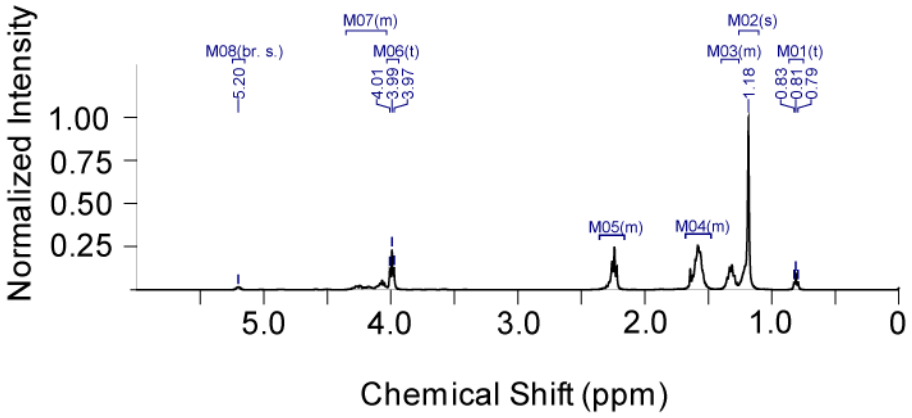

Figure S3. ^{1}H NMR of PGC-C18. (400 MHz, CDCl3)

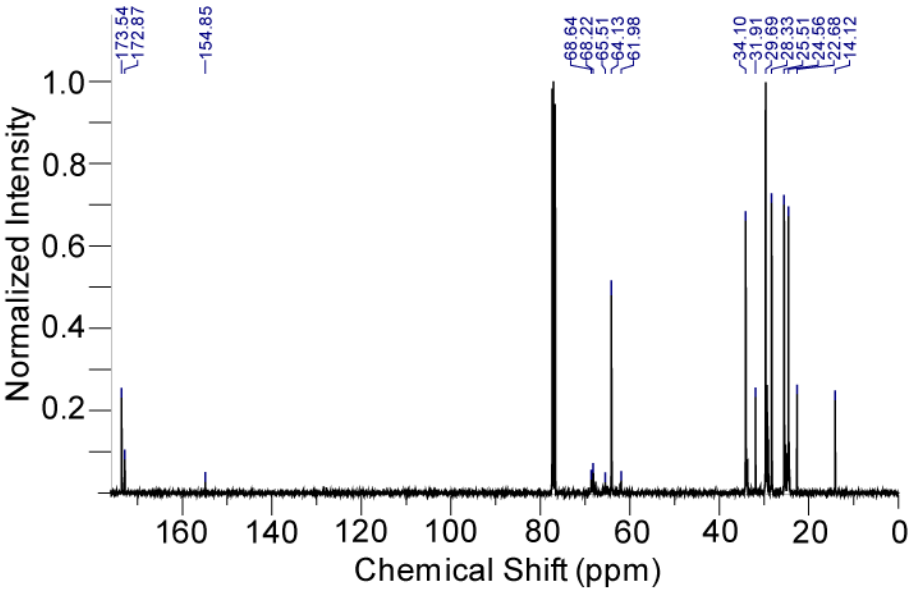

Figure S4. ^{13}C NMR of PGC-C18. (400 MHz, CDCl3)

4) Electrospinning:

	PCL:PGC-C18 copolymer blend ratios					
Polymer blend	*PCL alone*	*9:1*	*8:2*	*7:3*	*6:4*	*5:5*
PCL weight	*7%*					
PGC-C18 weight	*0*	*0.78%*	*1.75%*	*3.00%*	*4.67%*	*7.00%*
Applied potential	*8 kV*					
Grounded collector distance	*10 cm*					
Needle gauge	*20 gauge*					
Flow rate	*3 mL/hr*					
Electrospinning time	*85 seconds*	*78 seconds*	*69 seconds*	*60 seconds*	*52 seconds*	*43 seconds*

Table S1. PCL:PGC copolymer blends and electrospinning parameters. Electrospinning times were adjusted to electrospin 5 mg of polymer per batch of NP-NFM.

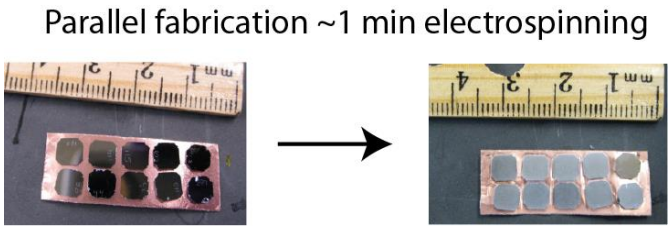

Figure S5. Images of nanopore chips before (left) and after (right) fabrication, showing parallelization of electrospinning technique. Up to 50 chips may be spun at once using our current apparatus.

5) Electrospun Mesh Morphology

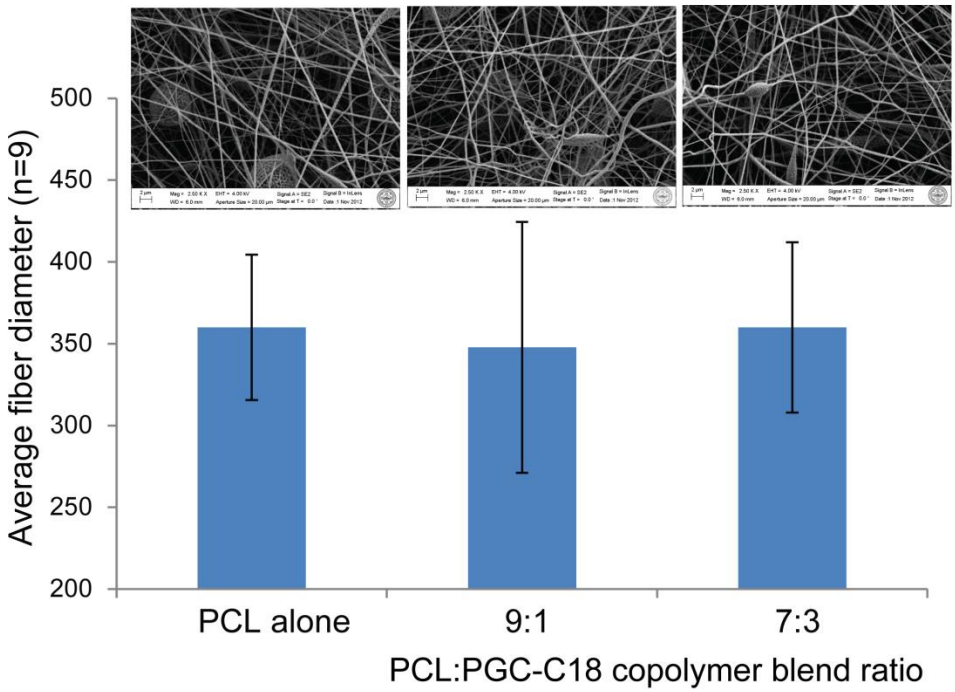

Figure S6. SEM images of 3 selected NFM copolymer blends with a constant PCL weight %. PGC-C18 content does not affect the physical properties (fiber diameter, mesh density, etc.) of the NFM. Fiber diameters for each blend range from ~250-450 nm. Representative fibers were chosen at random for each NFM copolymer blend. (Scale: 2 µm. Magnification: 2,500X. n=9, Avg±StDev, $p>0.05$ comparing each copolymer blend).

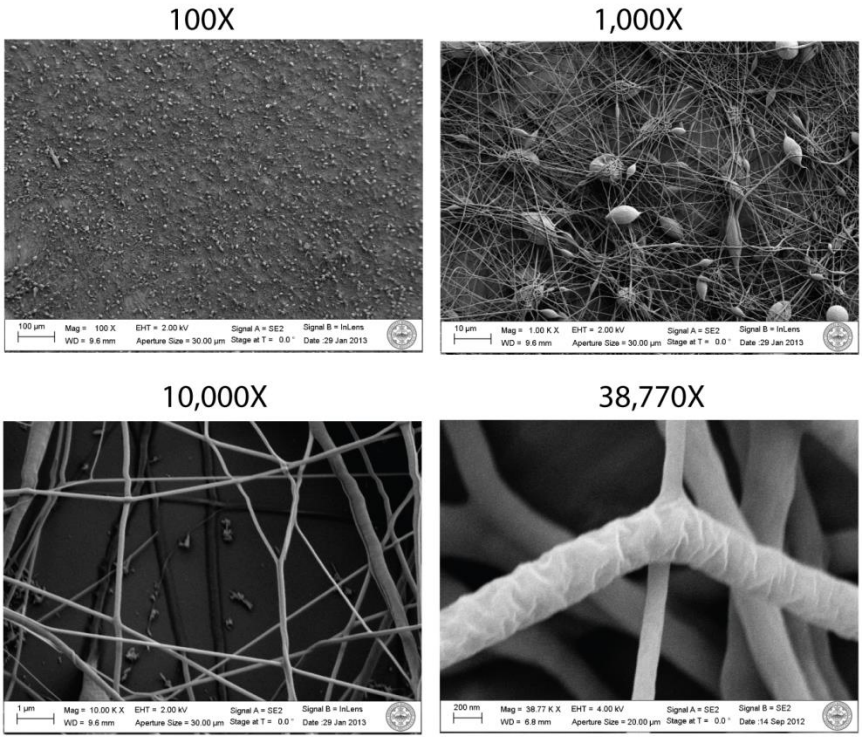

Figure S7. SEM images of a 7:3 PCL:PGC-C18 NP-NFM devices at 100X, 1,000X, 10,000X, and 38,770X. The scale bars are 100 µm, 10 µm, 1 µm, and 200 nm for the 100X, 1,000X, 10,000X, and 38,770X images, respectively. All NFM copolymer blends produce similar fiber diameters and bead morphology. Both micrometer and nanometer scale texture is produced by the NFMs allowing for the enhanced hydrophobicity observed in Figure 1. The SiN membrane is visible below approximately 3-4 layers of nanofibers (10,000X image) making the NFM approximately 1-2 µm thick.

6) DNA Translocation and Rinsing

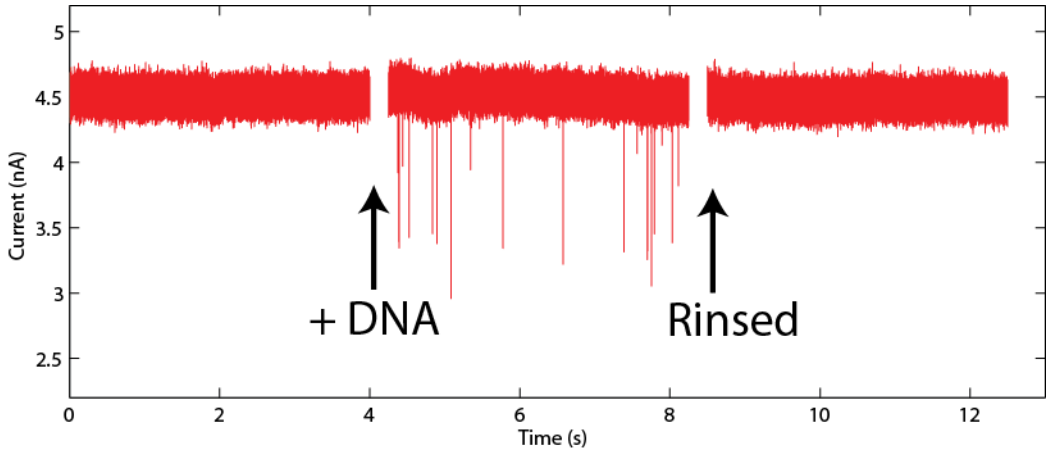

Figure S8. Current trace for a 4 nm pore at 500 mV, 1M:1M KCl with an 8:2 PCL:PGC-C18 NFM coating, filtered at 100 kHz. Initial trace (prior to adding DNA) shows a clean pore with a steady open pore current. After adding 1000 bp DNA, transient drops in current indicate the passage of individual molecules through the nanopore. The DNA was rinsed out with a 10x wash, returning the current trace to its original clean and open state.

7) NP-NFM Electrical Noise characterization

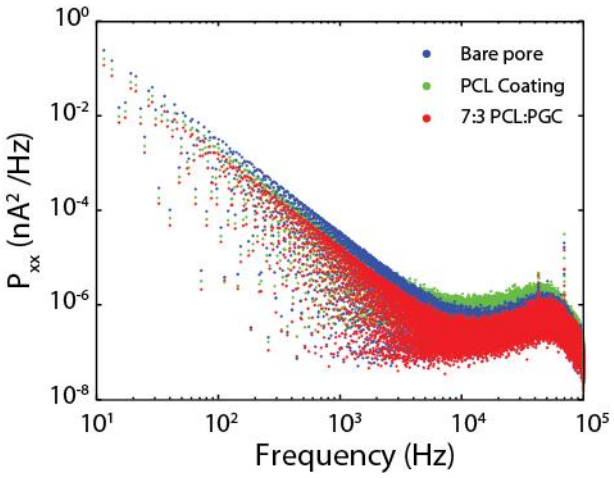

Figure S9. Power spectrum of noise in the same 4 nm nanopore at 300 mV, 1M:1M KCl, with three different NFM coating conditions: bare (blue), PCL only (green), and 7:3 PCL:PGC-C18 (red). All three power spectra are nearly identical, indicating that the addition of an NFM does not significantly change current noise in a solid-state nanopore.

8) Nanopore Blockage Level and Conductance

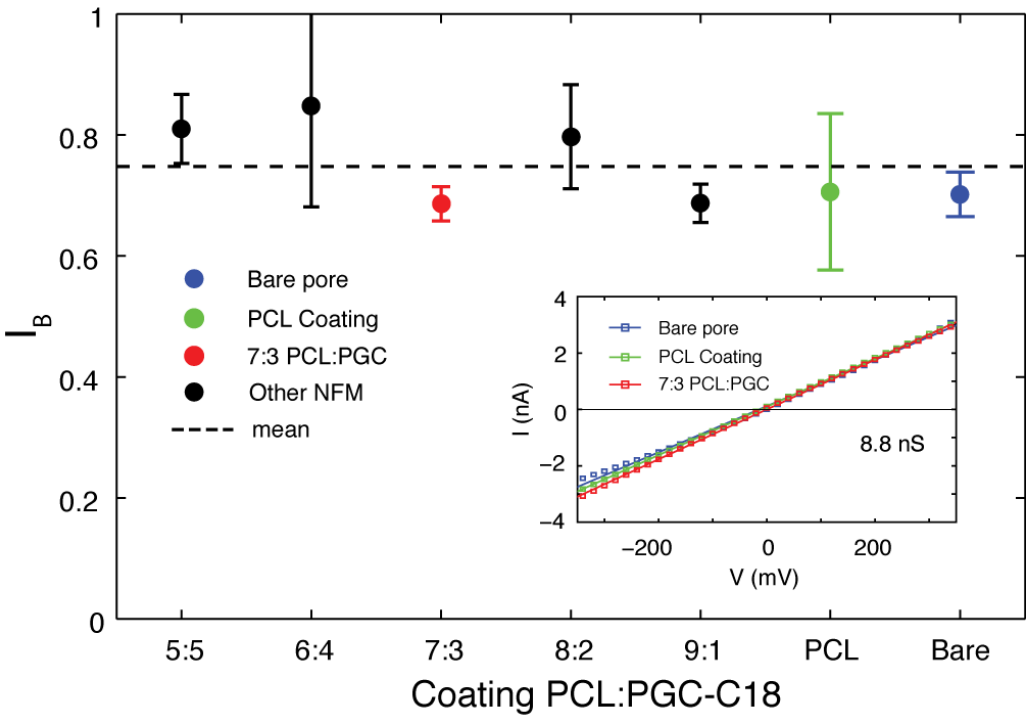

Figure S10. Effect of NFM coating on 1000 bp DNA translocation relative blockage level I_B (I_B= I_{block}/I_{open}) at 300 mV. In each case I_B was determined as a Gaussian fit to a histogram of event blockage levels, excluding folded events and collisions (Figure S10). Inset shows nanopore conductance for a single nanopore, measured bare, coated with PCL only, and coated with 7:3 PCL:PGC-C18. I_B points corresponding to the inset conductance measurements are colored accordingly.

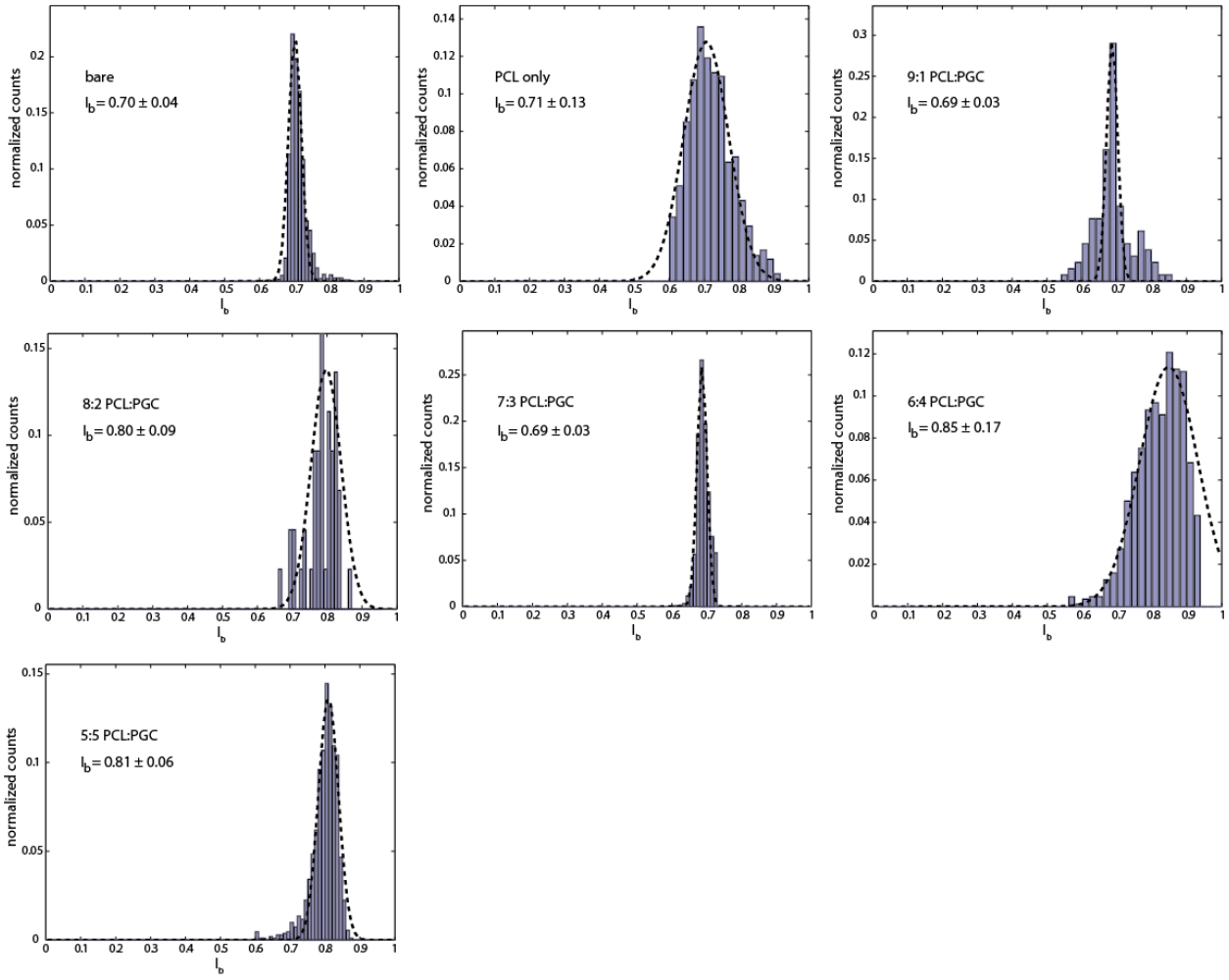

Figure S11. Gaussian fits to current blockage level I_B for 4 - 4.5 nm diameter nanopores at 300 mV, caused by translocation of 1000 bp DNA. Folded events and collisions were excluded wherever possible to simplify analysis.

9) Analysis methods of the dwell-time histograms of DNA translocations using various PCL:PGC-C18 copolymer blend ratios

We compared five methods of analysis for translocation dwell time, illustrated in Figure S12 using the data from Figure 3 in the main text as an example:

I) Most probable translocation time, t_{p_linear}, is defined for a linearly binned histogram of translocation times as the center of the most probable bin. Error is given by $\pm\frac{bin\ size}{2}$.

II) Characteristic translocation time, τ, is defined by an exponential decay fit to the tail of the linearly binned translocation time histogram: $PDF = Ae^{-\frac{t}{\tau_1}} + Be^{-\frac{t}{\tau_2}}$. Histograms for the bare pore at 300 mV and 500 mV were well-fit by a single exponential decay, whereas nearly all data sets for NFMs required two exponential decay terms (goodness of fit determined by R^2). Error is reported for a 95% confidence interval for this fit.

III) A variation on most probable translocation time, t_{p_log}, is defined as the Gaussian-fit mean of a log-binned histogram of translocation times. Error is reported for the 95% confidence interval for this fit.

IV) The mean translocation time, $\langle t_T \rangle$ is the numerical mean of all t_T with error defined by the standard deviation of the mean, $\pm\sigma_{SDOM}$.

V) Percent of events over 1 ms are counted, with counting error $\pm\,\sigma_{SDOM} \times 100\%$

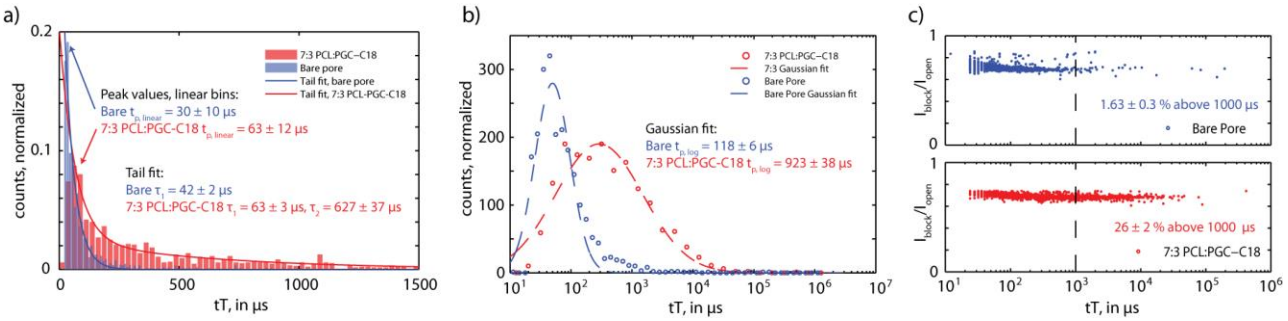

Figure S12. Depiction of analysis methods to characterize translocation time, shown for bare pore and 7:3 PCL:PGC-C18 NFM-coated pore at 300 mV, 1000 bp DNA. a) Methods I and II: Most probable translocation time (linear), t_{p_linear}, is taken from the distribution peak. Characteristic translocation times τ_i are given by exponential decay fits to distribution tails. b) Method III: Most probable translocation time (log), t_{p_log}, is determined by a Gaussian fit to the log-binned t_T. (Method IV, numerical mean, not shown) c) Method V: Events exceeding 1 ms (dotted line) are counted as a fraction of the data set.

Table S2 details the values of all metrics for the data sets used in the coatings study.

METHOD:			I	II		III	IV	V
Copolymer blend	**Voltage**	**# Events**	**t_{p_linear} (µs)**	**τ_1 (µs)**	**τ_2 (µs)**	**t_{p_log} (µs)**	**$\langle t_T \rangle$ (µs)**	**t_T > 1 ms (%)**
Bare pore	300	2141	30 ± 10	(42 ± 2)	42 ± 2	52 ± 3	118 ± 8	1.63 ± 0.3
PCL only	300	1025	75 ± 25	75 ± 5	878 ± 105	230 ± 72	937 ± 53	29 ± 1.7
9:1 PCL-PGC-C18	300	204	500 ± 100	330 ± 45	7293 ± 4400	739 ± 350	3550 ± 165	47 ± 6
7:3 PCL-PGC-C18	300	1672	62.5 ± 12.5	63 ± 3	627 ± 37	290 ± 55	923 ± 38	26 ± 1.2
6:4 PCL-PGC-C18	300	879	75 ± 25	68 ± 5	527 ± 54	204 ± 62	862 ± 53	30 ± 2
5:5 PCL-PGC-C18	300	1114	50 ± 10	44 ± 3	188 ± 11	98 ± 6	214 ± 16	2.5 ± 0.5
Bare pore	500	926	15 ± 10	(26 ± 2)	26 ± 2	22 ± 25	96 ± 9	1.2 ± 0.4
PCL only	500	1164	30 ± 10	58 ± 3	592 ± 45	281 ± 40	1110 ± 55	34 ± 1.7
9:1 PCL-PGC-C18	500	549	300 ± 100	325 ± 40	3670 ± 630	2051 ± 780	2072 ± 102	65 ± 3.4
8:2 PCL-PGC-C18	500	807	120 ± 40	181 ± 23	739 ± 94	338 ± 30	777 ± 28	20 ± 1.5
7:3 PCL-PGC-C18	500	1208	40 ± 40	-	384 ± 13	269 ± 34	505 ± 21	12 ± 1

Table S2. Values for each method of analysis of the characteristic translocation time for the various PCL:PGC-C18 copolymer blends tested, at both 300 and 500 mV,

Figure S13 graphically compares the performance of each metric as an indicator of change in translocation time due to the nanofiber mesh. All methods show a consistent trend of long translocation times for meshes of intermediate hydrophobicity, however only the exponential tail fit is able to capture both a population of extremely long events along with a population of shorter events which do not appear to interact with the mesh.

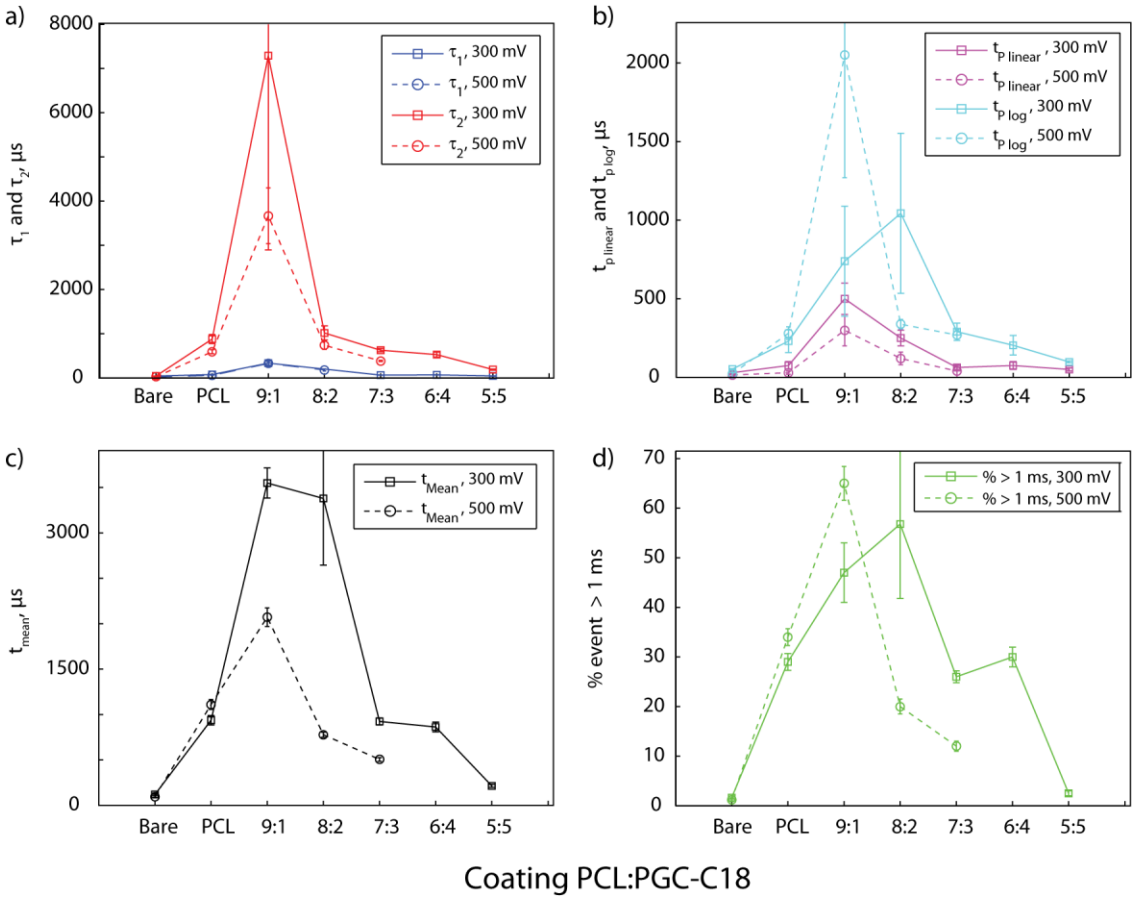

Figure S13. Methods for calculating translocation time, applied to bare pores and all coatings for 300 mV and 500 mV, 1000 bp DNA (data shown in Table S2). a) Characteristic translocation time τ (Method II). b) Most probable translocation times, t_{p_linear} and t_{p_log}. c) Mean translocation time t_{mean}. d) % of events over 1 ms.

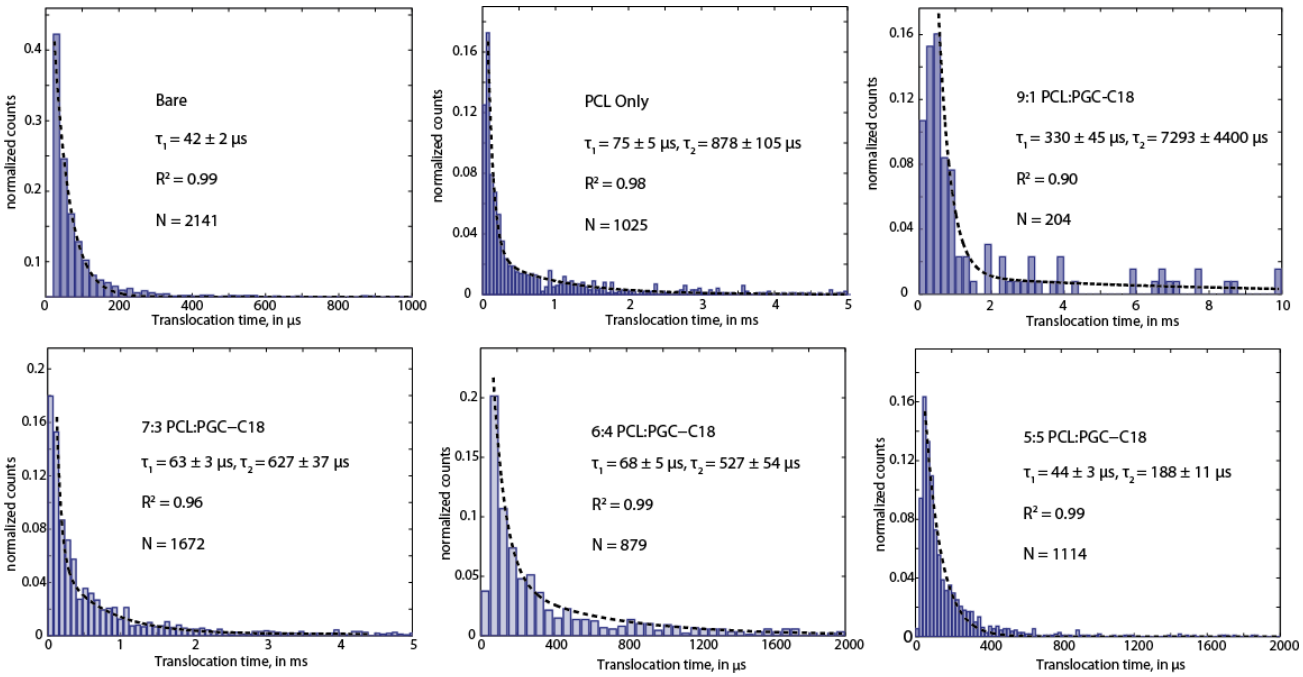

Figure S14. Exponential tail fits for translocation of 1000 bp DNA in 4-4.5 nm diameter nanopores at 300 mV. Tested coatings include a bare pore, PCL only, and 9:1, 8:2, 7:3, 6:4, and 5:5 PCL:PGC-C18 NFM coatings. Folded events and collisions were excluded where possible to simplify analysis.

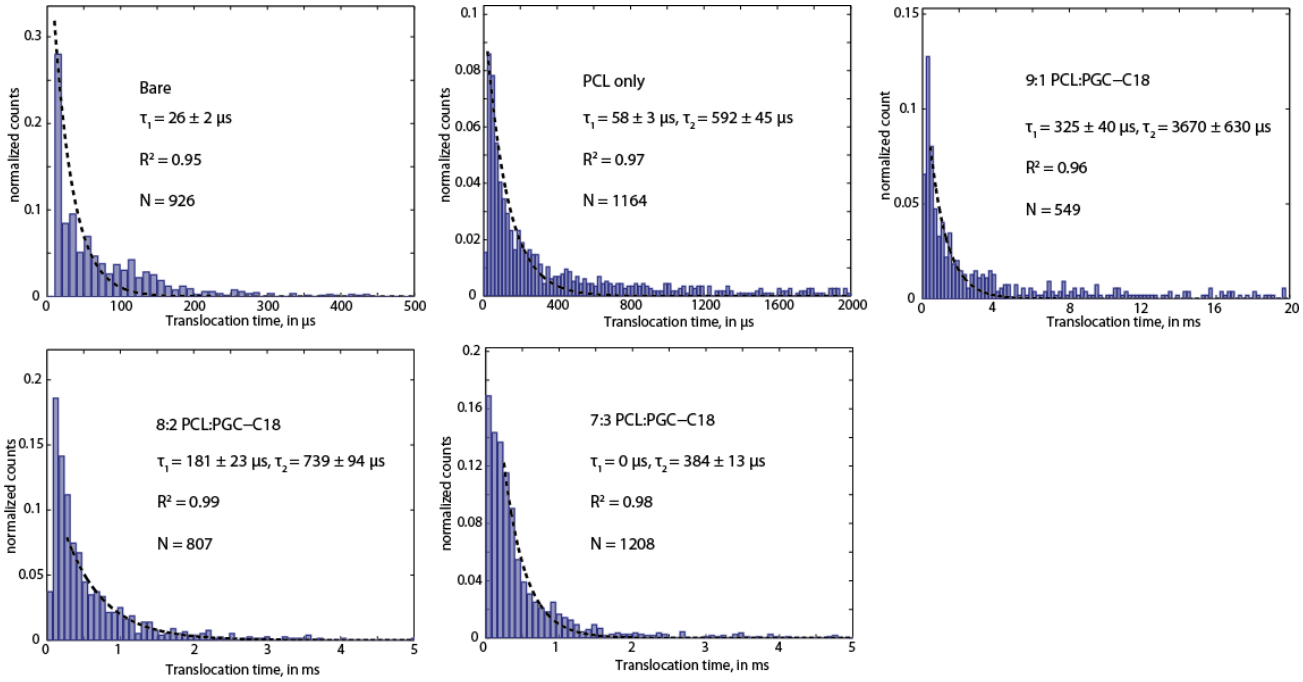

Figure S15. Exponential tail fits for translocation of 1000 bp DNA in 4-4.5 nm diameter nanopores at 500 mV. Tested coatings include a bare pore, PCL only, and 9:1, 8:2, and 7:3 PCL:PGC-C18 NFM coatings. Folded events and collisions were excluded wherever possible to simplify analysis.

10) DNA Lengths with NFM coating

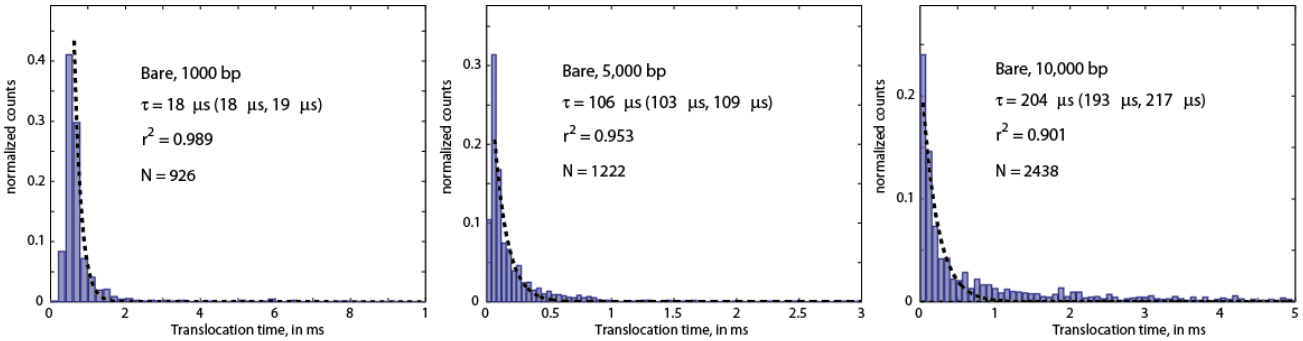

Figure S16. Exponential tail fits for translocation of 1 kbp, 5 kbp, and 10 kbp DNA in a bare 6 nm diameter nanopore at 500 mV. Folded events and collisions were excluded wherever possible to simplify analysis.

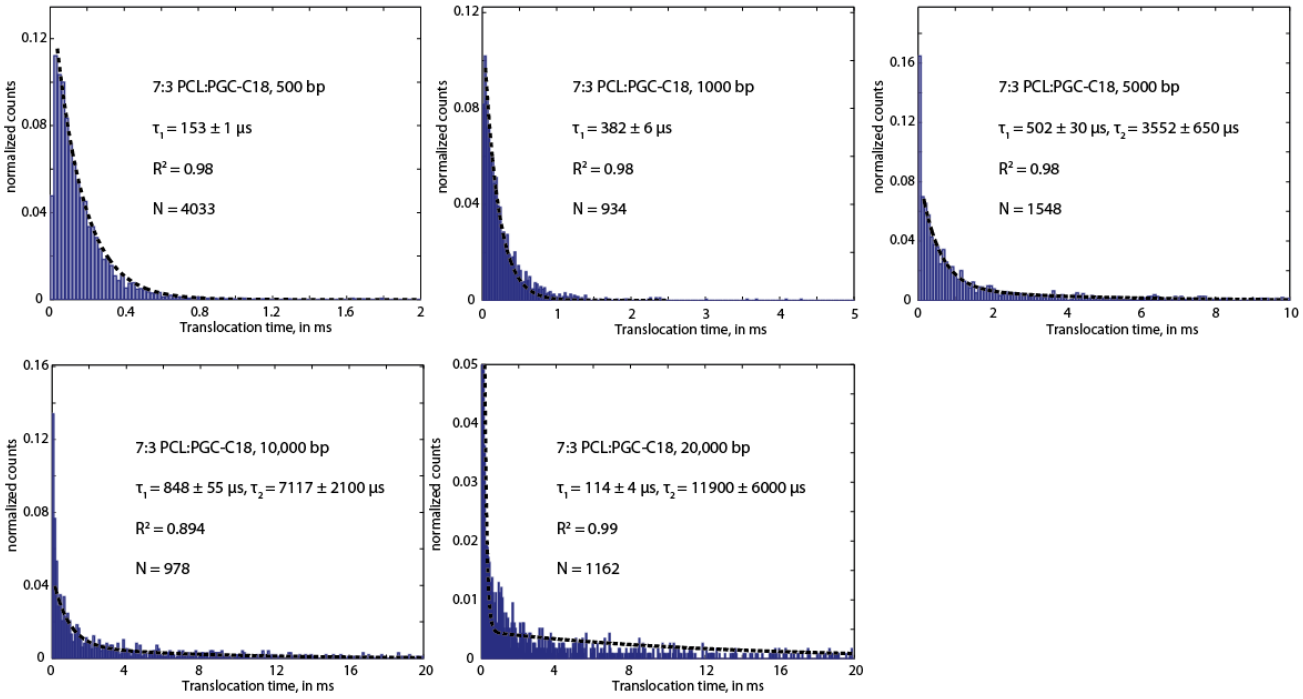

Figure S17. Exponential tail fits for translocation of 0.5 kbp, 1 kbp, 5 kbp, 10 kbp, and 20 kbp DNA in a 7:3 6 nm diameter nanopore at 500 mV. In the cases 5, 10, and 20 kbp, double exponential fits (indicated by *) were required to adequately fit the distributions. During the >12 hours of this experiment we observed a slow drift in the pore current (less than 5%); therefore in the manuscript Figure 5 we have normalized the blocked current by the mean blocked current to account for this unavoidable drift. Folded events and collisions were excluded wherever possible to simplify analysis.

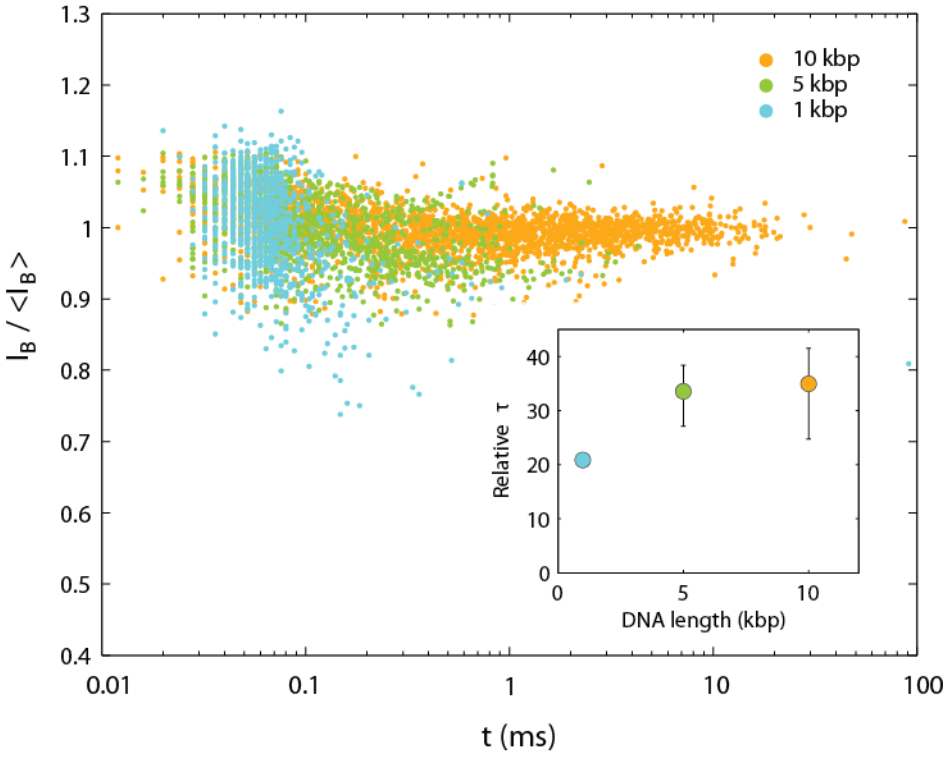

Figure S18. Event diagram for translocation of 1 kbp, 5 kbp, and 10 kbp DNA in a **bare** 6 nm diameter nanopore at 500 mV (fits in Figure S12). Inset shows relative τ for 1, 5, and 10 kbp in the 7:3 PCL:PGC-C18 coated nanopore (fits in Figure S13) normalized by this bare pore data. Although a slight increase in this retardation factor is observed with increasing length, there is little or no increase within the fit error (error bars for 1 kbp are smaller than marker).

References

(1) Wolinsky, J. B.; Ray, W. C.; Colson, Y. L.; Grinstaff, M. W. Macromolecules **2007**, 40, 7065.

(2) Yohe, S. T.; Colson, Y. L.; Grinstaff, M. W. Journal of the American Chemical Society **2012**, 134, 2016.

(3) Kim, M. J.; Wanunu, M.; Bell, D. C.; Meller, A. Advanced Materials **2006**, 18, 3149.

(4) Pham, Q. P.; Sharma, U.; Mikos, A. G. Biomacromolecules **2006**, 7, 2796.

(5) Yohe, S. T.; Freedman, J. D.; Falde, E. J.; Colson, Y. L.; Grinstaff, M. W. Advanced functional materials **2013**.

(6) Wanunu, M.; Sutin, J.; McNally, B.; Chow, A.; Meller, A. Biophys. J. **2008**, 95, 4716.

7) Meller, A.; Nivon, L.; Brandin, E.; Golovchenko, J.; Branton, D. Proceedings of the National Academy of Sciences **2000**, 97, 1079.